Coordinate expression and functional profiling identify an extracellular proteolytic signaling pathway

Ami S. Bhatt*, Alana Welm[†‡], Christopher J. Farady*, Maximiliano Vásquez[§], Keith Wilson[§], and Charles S. Craik*[¶]

*Department of Pharmaceutical Chemistry, University of California, 600 16th Street, San Francisco, CA 94158; [†]The G. W. Hooper Foundation, University of California, 513 Parnassus Avenue, San Francisco, CA 94153; and [§]PDL Biopharma, Inc., 34801 Campus Drive, Fremont, CA 94555

Edited by James A. Wells, University of California, San Francisco, CA, and approved February 6, 2007 (received for review July 30, 2006)

A multidisciplinary method combining transcriptional data, specificity profiling, and biological characterization of an enzyme may be used to predict novel substrates. By integrating protease substrate profiling with microarray gene coexpression data from nearly 2,000 human normal and cancerous tissue samples, three fundamental components of a protease-activated signaling pathway were identified. We find that MT-SP1 mediates extracellular signaling by regulating the local activation of the prometastatic growth factor MSP-1. We demonstrate MT-SP1 expression in peritoneal macrophages, and biochemical methods confirm the ability of MT-SP1 to cleave and activate pro-MSP-1 *in vitro* and in a cellular context. MT-SP1 induced the ability of MSP-1 to inhibit nitric oxide production in bone marrow macrophages. Addition of HAI-1 or an MT-SP1-specific antibody inhibitor blocked the proteolytic activation of MSP-1 at the cell surface of peritoneal macrophages. Taken together, our work indicates that MT-SP1 is sufficient for MSP-1 activation and that MT-SP1, MSP-1, and the previously shown MSP-1 tyrosine kinase receptor RON are required for peritoneal macrophage activation. This work shows that this triad of growth factor, growth factor activator protease, and growth factor receptor is a protease-activated signaling pathway. Individually, MT-SP1 and RON overexpression have been implicated in cancer progression and metastasis. Transcriptional coexpression of these genes suggests that this signaling pathway may be involved in several human cancers.

cancer | macrophage activation | protease substrate specificity | proteomics

Despite the successful physiological and biochemical characterization of many proteases, the vast majority of the >2% of the human genome that encodes proteases has yet to be functionally classified. Although many approaches demonstrate the sufficiency of a protease to cleave a given substrate, very few are able to address the physiological relevance of such *in vitro* findings. Cell-surface proteolysis is suggested to play a major role in cancer progression and metastasis through the processing of macromolecules important for regulating the extracellular environment. The cell-surface localization, high activity, and exquisite specificity of type II transmembrane serine proteases (TTSPs) suggest a role in outside-in signaling and interaction with the microenvironment. We elected to apply a multifaceted approach to identify physiologically relevant substrates of one prominent member of this family, membrane type serine protease 1 (MT-SP1/matriptase).

Members of the TTSP family, such as hepsin and MT-SP1, are highly expressed in many cancers, including those of the prostate, breast, colon, and ovary (1–9). Both overexpression and inhibition studies have supported the role of MT-SP1 in tumorigenesis and tumor growth. Targeted overexpression of MT-SP1 in squamous epithelia in mice results in skin-limited nodules of squamous cell carcinoma that become metastatic in the presence of the chemical carcinogen DMBA (10). Small molecule and macromolecular inhibitors of MT-SP1 have been developed and applied in a mouse model of cancer, resulting in growth suppression of androgen-independent prostate cancer xenografts (2, 11). Taken together, these findings suggest a role for MT-SP1 in cancer.

In this study, we sought to explore the mechanism of MT-SP1's activity in more detail. Although transcriptional coregulation has been reported between known pathway components, it has not been applied for the prediction of novel enzyme substrates (12, 13). Transcriptional profiling of nearly 2,000 human samples, including those from normal tissues, cancer cell lines, and 17 types of cancer tissue was performed to determine expression levels of MT-SP1, its candidate substrates, and its proposed endogenous inhibitor, the hepatocyte growth factor activator 1 (HAI-1) (14). Candidate substrates whose expression correlated with that of MT-SP1 in a statistically significant fashion were chosen for subsequent biochemical validation. These substrates were tested and validated in primary cells. Using this approach, we identified the cancer-associated growth factor macrophage-stimulating protein 1 (MSP-1) as a substrate of MT-SP1.

Results

Use of PS-SCL and Other Specificity Data to Guide Candidate Substrate Selection. Limited information on MT-SP1 substrate specificity was collected by using a complete diverse positionally scanned synthetic combinatorial library (PS-SCL) of synthetic substrates. The method can be used to identify consensus, nonprime side cleavage motifs for proteases (15). Our functional characterization of the binding specificity of MT-SP1 at the substrate-binding cleft is in accord with the information obtained from structural studies revealing trypsin-like specificity at the S1 position, a shallow pocket for small, hydrophobic residues at the S2 position, and an open negatively charged cavity at the S4 position, allowing for binding of a basic residue at P3 or P4 (16). Given the relative degeneracy of the specificity information obtained through biochemical profiling and structural studies, additional information was considered in the development of a consensus cleavage sequence. By using the specificity determinants obtained from the PS-SCL data and an alignment of known macromolecular substrates, a set of consensus sequences for MT-SP1 cleavage was deduced. The specificity of MT-SP1 was in fairly good agreement with the described cleavage sequence of the HGF-homolog, MSP-1 (Table 1).

Author contributions: A.S.B. and C.S.C. designed research; A.S.B. and A.W. performed research; A.S.B., A.W., C.J.F., M.V., and K.W. contributed new reagents/analytic tools; A.S.B., A.W., and C.S.C. analyzed data; and A.S.B. and C.S.C. wrote the paper.

The authors declare no conflict of interest.

This article is a PNAS Direct Submission.

Freely available online through the PNAS open access option.

Abbreviations: MT-SP1, membrane type serine protease 1; MSP-1, macrophage stimulating protein 1; HAI-1, hepatocyte growth factor activator inhibitor 1; TTSP, type two transmembrane serine protease; PS-SCL, positional scanning synthetic combinatorial library.

[‡]Present address: Department of Oncological Sciences, Huntsman Cancer Institute, University of Utah, Salt Lake City, UT 84112.

[¶]To whom correspondence should be addressed at: University of California, Genentech Hall, 600 16th Street, San Francisco, CA 94158-2517. E-mail: craik@cgl.ucsf.edu.

This article contains supporting information online at www.pnas.org/cgi/content/full/0606514104/DC1.

BIOCHEMISTRY

Table 1. Alignment of MSP-1 activation sequence with the predicted MT-SP1 cleavage sequence consensus

	P4	P3	P2	P1
Filaggrin	R	K	R	R
HGF/SF	K	Q	L	R
MT-SP1/matriptase	R	Q	A	R
PAR2	S	K	G	R
Trask/CDCP1/SIMA135	K	Q	S	R
uPA/urokinase	P	R	F	K
*P1-diverse PS-SCL	K/R	K/R	S > P > G > L	K/R
Phage Display	K/R vs. X	X vs. K/R	Small/hydrophobic	K/R
Crystal Structure	K/R vs. X	X vs. K/R	Small/hydrophobic	K/R
Consensus	K/R vs. S/P	Q vs. K/R	Small/hydrophobic	R > K
*MSP-1	S	K	L	R

Per standard notation, P1 is designated as the amino acid N-terminal to the scissile bond with P2 being the amino acid N-terminal to P1, etc. The P4 through P1 amino acids for known substrates of MT-SP1, P1-diverse PS-SCL data, phage display data, and crystallographic determinations are displayed. An MT-SP1 consensus cleavage sequence was derived from this information. The MSP-1 activation sequence is also presented. Asterisks indicate compiled PS-SCL data or MT-SP1 cleavage sequences determined by N-terminal sequencing in this work.

Transcriptional Profiling of Candidate MT-SP1 Substrates Demonstrates Two Candidate Proteins That Are Coexpressed with MT-SP1. To measure candidate gene RNA levels in human tissues and cell lines, tumor samples and cancer-derived cell lines were obtained from multiple sources. Tumor samples were obtained from the following tissue types: bladder, breast, cervical, colon, esophageal, head and neck, lung, ovarian, pancreatic, prostate, renal, stomach, testicular, and uterine cancers as well as Ewing's sarcoma, glioblastoma, and melanoma. Fifty-nine cancer cell lines, largely obtained from the American Type Culture Collection (Manassas, VA), were cultured *in vitro* and as SCID mouse xenografts. RNA was extracted from these samples, and RNA from 382 samples representing 86 types of nonpathogenic tissue was obtained from commercial sources. A single, custom microarray chip was designed to contain 400,000 perfect-match probes (≈59,000 probe sets). These arrays were then probed with biotinylated cDNA derived from the sample RNAs, and binding was quantitated by fluorescence. Genes of interest, such as described and predicted MT-SP1 substrates, the hepatocyte growth factor activator inhibitor 1 (HAI-1), and common cancer markers were chosen for further analysis. Both Pearson's product moment correlation coefficients and Spearman's rank-order correlation coefficients were calculated for all the given genes paired with MT-SP1. Bonferroni-corrected P values and false discovery rate P values are presented in supporting information (SI) Table 2. The data are summarized in Fig. 1, with statistical significance of the correlation established as $P < 0.05$ after Bonferroni correction or the false discovery rate correction (see *Methods* and *SI Appendix*). Significant correlations were not detected in cervical cancer, esophageal cancer, fetal tissues, head and neck cancer, Ewing's sarcoma, renal cancer, melanoma, or testicular cancer.

Expression of HAI-1 and MT-SP1 was significantly correlated in 13 of the tissue/cell line categories studied. The range of unadjusted P values calculated for the Pearson's product moment correlation coefficient range from 1.83×10^{-45} (HAI-1; normal tissues) to 0.994. The range of unadjusted P values calculated for the Spearman's rank-order correlation coefficient range from 5.85×10^{-34} (HAI-1; normal tissues) to 1. The most highly significant correlation detected was between HAI-1 and MT-SP1 in the aggregated sample of individually characterized normal body tissues.

This analysis showed that the expression of MT-SP1 and two of its previously described substrates, Trask and PAR2, was also significantly correlated in many tissue types. Interestingly, expression of the described MT-SP1 substrate HGF did not correlate well with MT-SP1 expression at the transcriptional level. Transcriptional expression of the HGF homolog, MSP-1, however, correlated well with expression of the protease in normal tissues and in certain cancers (Fig. 1). Furthermore, expression of the receptor for MSP-1, RON, very strongly correlated with MT-SP1 expression. Although RON has a fairly narrow expression pattern in normal tissues, including terminally differentiated macrophages, keratinocytes, several types of columnar epithelium, and osteoclasts (17), our data demonstrated aberrant receptor expression in certain cancer tissues. MT-SP1 and RON transcript levels were correlated in several tissue types

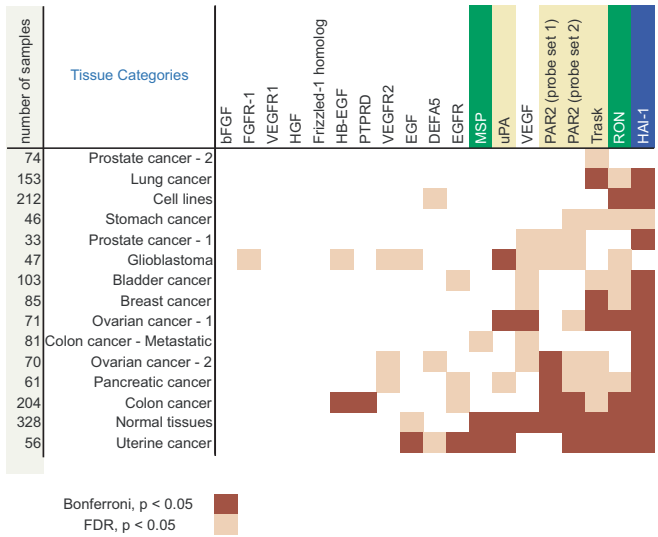

Fig. 1. Correlational cluster diagram of MT-SP1 and associated proteins. Transcriptional profiling of 19 genes was performed for nearly 2,000 samples from cell lines, normal tissues, and cancer tissues. Pearson's and Spearman's correlation coefficients were calculated for each gene paired with MT-SP1. Associated P values were also calculated and corrected by using the Bonferroni correction method (highly specific) and the false discovery rate (FDR) method (highly sensitive). Significantly correlated gene pairs (adjusted $P < 0.05$) are indicated by shading. Tissue categories without any significant correlations are not displayed. All correlations determined to be significant by using the Bonferroni method (darker shading) are significant by using the FDR method (lighter shading). Transcript levels of HAI-1, the proposed endogenous inhibitor of MT-SP1, are significantly correlated with transcript levels of MT-SP1 in the largest proportion of tissues.

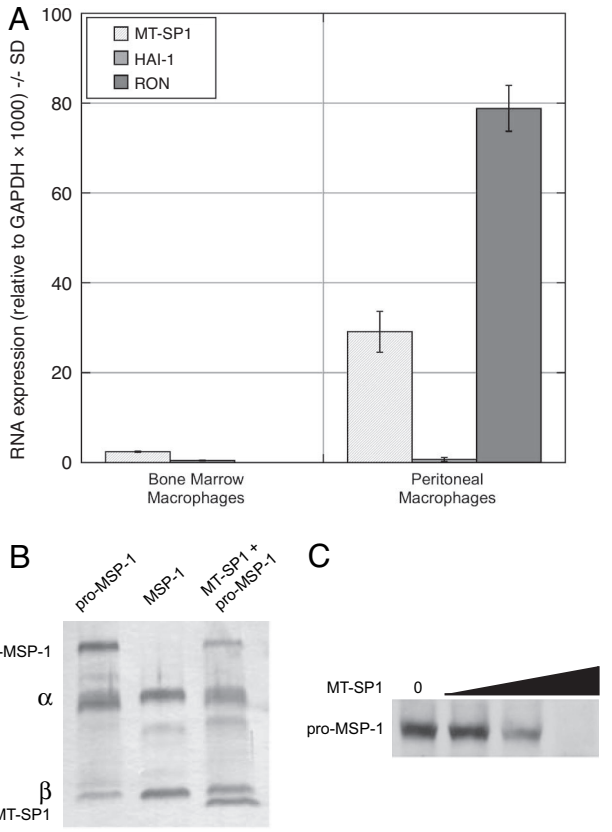

Fig. 2. MT-SP1 and RON, but not HAI-1, are expressed in peritoneal macrophages, and MT-SP1 cleaves MSP-1 at the activation site. (*A*) TaqMan was performed to determine MT-SP1, RON, and HAI-1 expression in primary mouse bone marrow-derived macrophages and peritoneal macrophages. MT-SP1 and RON are expressed at levels at least 10-fold greater in peritoneal macrophages than in bone marrow-derived macrophages. HAI-1 is not expressed in either cell type. (*B*) One hundred nanomolar MT-SP1 was incubated with 200 ng of pro-MSP-1 for 30 min at 37°C and then separated by SDS/PAGE. Approximately 50% of pro-MSP-1 is processed into the active α-β heterodimer in this time, as judged by silver stain. Decrease of the intensity of the pro-MSP-1 band is accompanied by a concomitant increase in the intensity of the band representing the β chain of MSP-1. (*C*) MT-SP1 activates pro-MSP-1 in a dose-dependent manner as is shown by disappearance of the full-length pro-MSP-1 by immunoblot (from left to right: 1 nM, 10 nM, and 100 nM).

with coexpression strength on par with MT-SP1/Trask and MT-SP1/HAI-1. The MT-SP1/MSP-1/RON interaction was chosen for subsequent biochemical validation.

MT-SP1 Is Present on the Cell Surface of Peritoneal Macrophages. Quantitative RT-PCR (Fig. 2) and immunoblotting (data not shown) demonstrated the expression of both MT-SP1 and RON in mouse peritoneal macrophages at levels >10-fold higher than in bone marrow-derived macrophages (Fig. 2). The endogenous inhibitor of MT-SP1, HAI-1, was not highly expressed in either cell type. MSP-1 and RON were originally described as important components of signaling cascades at the surface of certain populations of mature and differentiated macrophages. Previous studies have identified a cell-surface, trypsin-fold serine protease activity on macrophages that activates MSP-1, potentiating MSP-1 binding to RON and subsequent macrophage activation (18–20).

Cell Surface-Bound MT-SP1 Can Cleave the Predicted Substrate pro-MSP-1. We investigated whether MT-SP1 could activate MSP-1 for several reasons: (*i*) MSP-1 requires proteolytic activation to

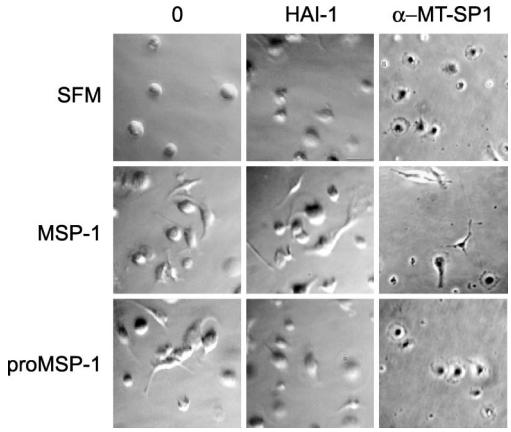

Fig. 3. MT-SP1-activated MSP-1 induces macrophage activation and morphology change. Primary mouse peritoneal macrophages were serum-starved and incubated in serum-free medium (SFM) in the absence or presence of 50 ng/ml MSP-1, 50 ng/ml pro-MSP-1, 40 nM HAI-1, and 400 nM anti-MT-SP1 antibody as indicated for 4 h. Upon treatment with MSP-1 or pro-MSP-1, the macrophages undergo a characteristic morphological change demonstrated by the development of an elongated shape and spiny protrusions. HAI-1 or anti-MT-SP1 antibody inhibition of endogenous MT-SP1 proteolytic activity abrogates the ability of pro-MSP-1 to induce this morphological change.

bind and activate its receptor RON (18–21) (*ii*) MSP-1 contains the consensus sequence for cleavage by MT-SP1 (Table 1), and (*iii*) MT-SP1 and RON are coexpressed in both peritoneal macrophages and cancer tissues, consistent with previous observations that MSP-1 is activated at the surface of cells that respond to MSP-1 (20). Activation of MSP-1 is the result of proteolysis C-terminal to R^{483} (21). The specificity determinant N-terminal to R^{483} is the peptide sequence SKLR (P4-P1) (22), and is in agreement with the PS-SCL results for MT-SP1 (Table 1). MT-SP1 cleaved pro-MSP-1 into two major fragments, which corresponded to the α and β chains of the mature MSP-1 (Fig. 2). Cleavage at R^{483} was confirmed by N-terminal sequencing of the β chain (data not shown). The dose-dependence of this cleavage event was established by analyzing pro-MSP-1 cleavage over a 1,000-fold concentration range. Cleavage of MSP into the α and β chains was detectable at concentrations of protease as low as 1 nM, with nearly complete activation of pro-MSP-1 by 100 nM MT-SP1 within 1 h at 37°C. Activation of RON at R^{309} after the specificity determinant RRRR (P4-P1) was also demonstrated by the nearly complete processing of single chain RON into the mature α/β complex by MT-SP1 (data not shown).

MSP-1 Activation by MT-SP1 Results in Macrophage Morphology Changes and Inhibition of Nitric Oxide Production by Macrophages. The cleavage of MSP-1 by MT-SP1 was then tested in primary cells in culture. Macrophages respond to MSP-1 via RON activation, leading to changes in cell shape and increased migration, as well as an inhibition of nitric oxide production (23–25). We found that primary mouse peritoneal macrophages, but not primary mouse bone marrow macrophages, underwent a characteristic shape change upon activation by MSP-1 (Fig. 3) (25). The effects of the endogenous MT-SP1 inhibitor, HAI-1, and a highly specific MT-SP1 antibody inhibitor (Fig. 3) were studied. The morphology change in response to MSP-1 was independent of HAI-1 or anti-MT-SP1 antibody presence. Both inhibitors were used at concentrations 10-fold over the reported K_i. Cell surface-bound MT-SP1 converted pro-MSP-1 into its biologically active form, and cells underwent morphology change when incubated with pro-MSP-1 in the absence of HAI-1 or the anti-MT-SP1 antibody. Addition of a specific inhibitor of MT-SP1, either HAI-1 or the anti-MT-SP1 antibody, prevented

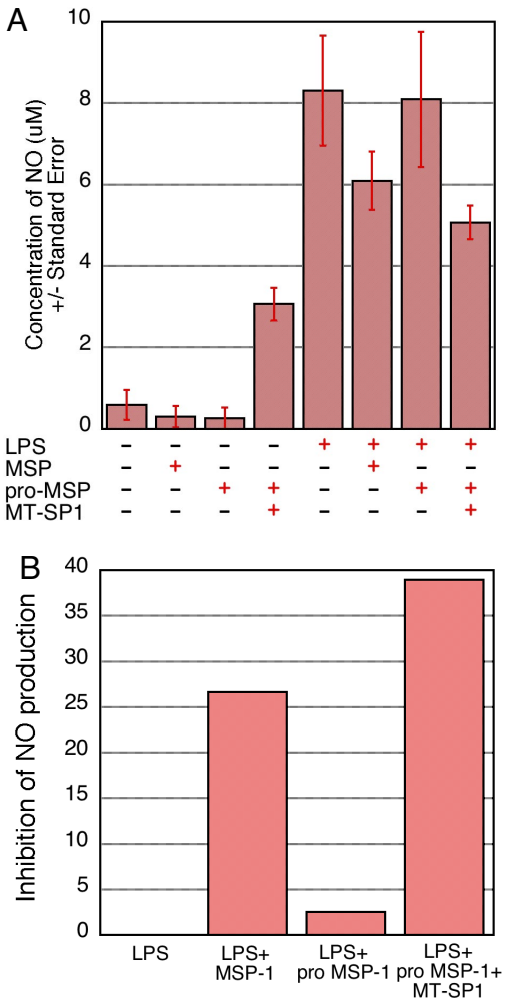

Fig. 4. MT-SP1 activated MSP-1 inhibits LPS-induced nitric oxide production in macrophages. Mouse bone marrow macrophages were isolated and cultured in 24-well plates. Nitric oxide production was measured by the Griess reaction. The macrophages exhibit a robust nitric oxide production response to the positive control of 1 μg/ml LPS. (*A*) From left to right, the histogram represents cell cultured with (*i*) medium alone, (*ii*) 10 ng/ml MSP-1, (*iii*) 10 ng/ml pro-MSP-1, (*iv*) 10 ng/ml pro-MSP-1 plus 10 nM MT-SP1, (*v*) 1 μg/ml LPS, (*vi*) 1 μg/ml LPS plus 10 ng/ml MSP-1, (*vii*) 1 μg/ml LPS plus 10 ng/ml pro-MSP-1, and (*viii*) 10 ng/ml pro-MSP-1 plus 10 nM MT-SP1 plus 1 μg/ml LPS. The experiment was repeated twice in triplicate, and the data from these experiments were averaged and are reported $\pm$SE. (*B*) The data are also presented as percent inhibition of NO production as a function of sample conditions.

macrophage activation despite the presence of pro-MSP-1. These data indicate that MT-SP1, present on the peritoneal macrophage cell surface, is responsible for the activation of pro-MSP-1.

Another measure of macrophage response to MSP-1 is inhibition of LPS-induced nitric oxide production. MSP-1 is a strong attenuator of bone marrow macrophage nitric oxide production in its activated form but does not exhibit this property in its pro-form (23). Primary mouse bone marrow macrophages showed a robust production of nitric oxide in response to LPS (Fig. 4*A*). As expected, pro-MSP-1 alone did not inhibit this response. At baseline, the addition of MT-SP1 alone stimulated production of NO. This is likely secondary to LPS contamination in the recombinant MT-SP1 as it is produced in *Escherichia coli*. However, upon activation of pro-MSP-1 with exogenously added MT-SP1, there was a nearly 40% inhibition of LPS-induced nitric oxide production, commensurate with that achieved with MSP-1 (Fig. 4).

Pro-MSP-1 is thus converted to its bioactive form by MT-SP1, as measured by both macrophage morphology change and inhibition of macrophage nitric oxide production. Furthermore, endogenous MT-SP1 is likely to be responsible for pro-MSP-1 activation on the surface of peritoneal macrophages.

Discussion

Determining the physiological role of orphan proteases has been a long-standing challenge. Many successful approaches have been recently reported by using affinity-tagged mass spectrometric labeling of newly cleaved substrates and through the use of specific macromolecular inhibitors of proteases to identify key components of important cellular pathways (26, 27). Using a strategy combining specificity profiling, transcriptional data, and biochemical enzyme characterization, we have identified a protease (MT-SP1/matriptase), its growth factor substrate (MSP-1), and the corresponding growth factor receptor (RON) as basic components of a cell-stimulatory cascade.

Considering that MT-SP1 could play a significant biochemical role in mediating signaling by processing cancer-related proteins *in vivo*, we hypothesized that these signaling proteins would likely be coexpressed with MT-SP1. To test this hypothesis, a group of candidate genes were chosen whose expression correlated with that of MT-SP1 in cancer tissues. The protein products of these genes were then analyzed for accessible MT-SP1 cleavage motifs. Finally, candidate substrates that were coexpressed with MT-SP1 and had accessible cleavage motifs were validated *in vitro* and in cell-based assays. The coexpression of MT-SP1 with its proposed endogenous inhibitor, HAI-1, provided authentication of our approach. The biological interaction between HAI-1 and MT-SP1 has previously been described in human breast milk (14). Further studies support the interaction of HAI-1 and MT-SP1 in breast cancer tissues, because protein levels of the protease-inhibitor pair are well correlated by immunohistochemistry in a majority of 330 node-negative breast cancer tissue samples (5). Recent work has suggested a role for HAI-1 in both inhibition of MT-SP1 and trafficking of MT-SP1 to the cell surface (28). In our study, MT-SP1 and HAI-1 transcript levels were significantly correlated in a majority of the cancerous tissues examined. This strong correlation suggests that HAI-1 may act as an inhibitor of MT-SP1 in several other types of cancers in addition to the originally shown interaction in breast milk and breast cancer tissue.

Coexpression analysis showed that transcript levels of MT-SP1 and three of its previously described substrates, uPA, PAR2, and Trask, were also significantly correlated in many tissue types. The G protein-coupled receptor PAR2 and the plasminogen activator uPA are both activated by MT-SP1-mediated proteolysis *in vitro*, and some *in vivo* evidence exists to support the physiologic role of MT-SP1 in activating these proteins (29). Recently, Trask/CDCP1/SIMA135, a mitotic substrate of src kinases, was shown to be an endogenous substrate of MT-SP1 (30). Along with HAI-1, Trask was one of the most tightly coregulated proteins identified in the present study. Thus, several PS-SCL-identified substrates of MT-SP1 were coexpressed with MT-SP1, supporting their involvement in MT-SP1-modulated pathways *in vivo*. These data also provide further authentication of the combined substrate specificity/coexpression method for identification of protease substrates. MT-SP1 and a subset of its substrates/inhibitors are coexpressed, and this relationship may be partially generalized to other MT-SP1 substrates and other enzyme-substrate pairs. It is important to note, however, that this approach may not be fully generalized, given that many substrates are expressed distally from the site of enzyme production.

The finding that MT-SP1 and MSP-1 were highly coexpressed supports their physiologic relevance as an enzyme-substrate pair. The interaction was studied in a cell-based system of peritoneal macrophages. We demonstrated that MT-SP1 is expressed on peritoneal macrophages that respond to MSP-1. Although the transcriptional data suggest that HAI-1 and MT-SP1 are often coexpressed, the interaction between HAI-1 and MT-SP1 is likely complex. Peritoneal macrophages represented an ideal system for the study of MT-SP1 because they are primary cells and lack HAI-1, thereby eliminating a possible confounding element to the analysis of cell-based inhibition assays. The exact role of HAI-1 in processes, such as inhibition and trafficking of MT-SP1, however, remains to be determined.

The substrate-specificity profiling data for MT-SP1 is in agreement with its ability to cleave the activation sequence of MSP-1, and this was confirmed *in vitro*. Further experiments demonstrated that cell surface-bound MT-SP1 on peritoneal macrophages activates MSP-1 into its bioactive form and that this constitutive activation could be blocked by the addition of exogenous HAI-1 or a specific antibody inhibitor of MT-SP1. Activation of RON by MSP-1 led to alteration in peritoneal macrophage cell morphology and important downstream biochemical changes such as modulation of NO production in bone marrow-derived macrophages.

Although RON activation by MSP-1 has been thoroughly described in macrophages, resulting in myriad effects ranging from macrophage activation to chemotaxis to proliferation (19), this signaling pathway is also important elsewhere. For example, overexpression of either MT-SP1 or RON, leads to spontaneous tumor formation in mouse models (31, 32). Given this and the data supporting MT-SP1, MSP-1, and RON expression in various cancer tissues, we suggest that this pathway may be important in tumor development, maintenance, and/or progression. MT-SP1, MSP-1, and RON have all been established as cancer-associated molecules (2, 17, 33, 34). We suggest that cancer cells may "hijack" this signaling pathway by increasing coordinate expression of MT-SP1, MSP-1, and RON to drive proliferation and migration, two fundamental traits of transformed cells. The components of this extracellular proteolytic signaling pathway are involved in macrophage activation and are coexpressed in several tumors, suggesting that the cascade may play a critical biological role in certain cell types and many cancer tissues. Their participation in activation of macrophages is particularly interesting, given the association between cancer progression and inflammation (35). The pathway described here may, indeed, have clinical significance, as suggested by a recent study showing that tumors overexpressing MSP-1/MT-SP1/RON are significantly more metastatic than the control group in which only a subset of these genes are expressed (34).

Although this work suggests the sufficiency and importance of MT-SP1 for the activation of MSP-1, MT-SP1 is a member of a much larger family of TTSPs. In certain tissues, these TTSPs may exhibit redundancy of function and may substitute for MT-SP1 in this newly described pathway. Thus, we propose that membrane associated serine proteases, such as, but not limited to, MT-SP1, represent a previously uncharacterized conceptual class of upstream regulators of growth factor activity and thus as catalysts in the initiation of outside-in signaling.

Methods

PS-SCL. Recombinant MT-SP1 was prepared as described (11), and substrate specificity of MT-SP1 was determined by using conditions described in refs. 15 and 36. For further details, please see *SI Methods*.

Tumor Samples, RNA Preparation, and Hybridization to Custom DNA Microarrays. Tumor samples and cell lines were obtained from multiple sources with IRB approval for all tumor samples used in this study. Breast, prostate, and ovarian cancer specimens were obtained from two independent research trials and were therefore analyzed separately and are referred to as trials 1 and 2. Total RNA from nonpathogenic human tissues and organs was obtained commercially (Clontech, Palo Alto, CA; Invitrogen, Carlsbad, CA) or was isolated from fresh-frozen cadaveric samples (Zoion Diagnostics, Shrewsbury, MA) from trauma victims. The details of the tissue samples used and microarray design are more thoroughly described in *SI Methods*.

Quantitative RT-PCR. RNA was extracted from both mouse bone marrow macrophages and peritoneal macrophages by using TRIzol reagent as described elsewhere in this manuscript. The following TaqMan primers were purchased: (Mm00436365_m1 (RON), Mm00487858_m1 (MT-SP1), Mm00444186_m1 (HAI-1) (Applied Biosystems, Foster City, CA). All reactions were performed with Universal PCR Master Mix (Applied Biosystems) using the AB 7300 Real Time PCR system and were monitored over 40 cycles according to manufacturer's recommendations.

Statistical Analysis. Gene expression data were collected for MT-SP1, known substrates, putative substrates, and control genes. To determine the level of correlation of MT-SP1 with these candidate genes, two statistical methods were used. All calculations were performed by using Microsoft Excel or the statistical shareware "R" and are detailed in *SI Appendix*. Pearson's product moment correlation coefficients, Spearman's rank-order correlation coefficients, and associated *P* values were calculated. These *P* values were then corrected by using both the Bonferroni correction and the false discovery rate correction to account for making multiple comparisons (37). Correlation significance was stratified based on the calculated *P* values for both Pearson's and Spearman's correlation calculations. Correlation coefficient pairs and tissue types were clustered and presented in a diagrammatic format. Gene pairs are color coded according to level of significance and sign of the correlation, as described in the figure legend.

Isolation and Culture of Mouse Bone Marrow and Resident Peritoneal Macrophages. Mouse bone marrow macrophages were isolated by flushing the marrow of collected mouse femurs with DMEM and by selection *in vitro* (detailed description in *SI Methods*). Resident peritoneal macrophages were collected from mice by using 10 ml of DMEM or RPMI medium 1640 for peritoneal lavage. Cells were collected by centrifugation and were plated in either DMEM or RPMI medium 1640 with 10% FBS and 1× Pen/Strep. The yield was $\approx 5 \times 10^5$ cells per mouse.

Recombinant MSP-1 Cleavage Reactions. Recombinant human MT-SP1 catalytic domain was prepared and active site titrated as described (11). Recombinant pro-MSP-1 and mature MSP-1 was purchased from R & D Systems (Minneapolis, MN). Briefly, 200 ng of pro-MSP-1 or mature MSP-1 was incubated in the presence or absence of 100 nM MT-SP1 for 30 min at 37°C. This corresponds to a molar ratio of substrate to enzyme of 1.25:1. The products were then separated by SDS/PAGE on 4–20% Tris-glycine gels (Invitrogen) and either silver stained or blotted onto PVDF for microsequencing or nitrocellulose for immunoblotting. N-terminal sequencing of MSP-1 cleavage products was carried out at the University of California Molecular Structure Facility (Davis, CA).

Macrophage Morphology Change Assays. Resident peritoneal mouse macrophages were plated at a density of $\approx 2 \times 10^4$ cells per well in sterile nontissue culture, 24-well plates and cultured in serum-free DMEM overnight. Recombinant MSP-1, pro-MSP-1, HAI-1, and the MT-SP1-specific antibody inhibitor were added to 750 μl of DMEM as indicated in Fig. 3. The antibody

inhibitor was prepared as described and used at a final assay concentration of 400 nM (38). MSP-1 and pro-MSP-1 were used at 50 ng/ml, and HAI-1 was used at 40 nM. Four hundred seventy-five microliters of this culture medium was then applied to the serum-starved cells. After a 1-h incubation at 37°C with 5% CO_2 injection, the cells were analyzed by inverted microscopy, and representative pictures were taken. The experiment was repeated three independent times, and microscopic image acquisition and analysis was blinded.

Testing MT-SP-1 Cleaved MSP-1 for Bioactivity in Nitric Oxide Production Assays. Bone marrow mouse macrophages were isolated as described above and were plated at a density of $\approx 5 \times 10^5$ cells per well in 24-well plates and cultured in serum-free DMEM for 2 h. Recombinant rhMSP-1, pro-MSP-1, MT-SP1, and LPS were added to 750 μl of DMEM as indicated in Fig. 4 and sterile-filtered with a 0.22-μm syringe-driven filter unit (Millipore, Billerica, MA). The final concentration of MSP-1 and pro-MSP-1 was 10 ng/ml, the final concentration of MT-SP1 was 10 nM, and the final LPS concentration was 1 μg/ml. This medium was then added to the cells, and they were cultured for 24 h. After 24 h, nitric oxide production was measured by using the Griess reaction (23). The experiment was performed twice in triplicate. The data were combined and are represented as the average nitric oxide production, with the standard error indicated (Fig. 4*A*). The data are also depicted by condition type as a function of inhibition of NO production (Fig. 4*B*). Percent inhibition of NO production was calculated for each condition as follows. LPS-mediated NO production was established as 0% inhibition. Percent inhibition of NO production for each condition was then calculated as the difference of 100% inhibition and the percentage of NO production in the test sample versus the LPS-alone condition.

We thank R. Roydasgupta and J. Fridlyand of the University of California Comprehensive Cancer Center (San Francisco, CA) for advice and guidance in the use of statistical methods and J. M. Bishop for the use of reagents and facilities at the G. W. Hooper Foundation. This work was supported by the University of California Chancellor's Fellowship, an ARCS Foundation Fellowship, the National Institutes of Health (NIH) Medical Scientist Training Grant (to A.S.B.), a Department of Defense Breast Cancer Research Fellowship (to C.J.F.), and an NIH Program Project Grant (to C.S.C.).

1. Cao J, Zheng S, Zheng L, Cai X, Zhang Y, Geng L, Fang Y (2001) *Chin Med J (English)* 114:726–730.
2. Galkin AV, Mullen L, Fox WD, Brown J, Duncan D, Moreno O, Madison EL, Agus DB (2004) *Prostate* 61:228–235.
3. Hoang CD, D'Cunha J, Kratzke MG, Casmey CE, Frizelle SP, Maddaus MA, Kratzke RA (2004) *Chest* 125:1843–1852.
4. Johnson MD, Oberst MD, Lin CY, Dickson RB (2003) *Exp Rev Mol Diagn* 3:331–338.
5. Kang JY, Dolled-Filhart M, Ocal IT, Singh B, Lin CY, Dickson RB, Rimm DL, Camp RL (2003) *Cancer Res* 63:1101–1105.
6. Oberst MD, Johnson MD, Dickson RB, Lin CY, Singh B, Stewart M, Williams A, al-Nafussi A, Smyth JF, Gabra H, Sellar GC (2002) *Clin Cancer Res* 8:1101–1107.
7. Riddick AC, Shukla CJ, Pennington CJ, Bass R, Nuttall RK, Hogan A, Sethia KK, Ellis V, Collins AT, Maitland NJ, *et al.* (2005) *Br J Cancer* 92:2171–2180.
8. Santin AD, Cane S, Bellone S, Bignotti E, Palmieri M, De Las Casas LE, Anfossi S, Roman JJ, O'Brien T, Pecorelli S (2003) *Cancer* 98:1898–1904.
9. Dhanasekaran SM, Barrette TR, Ghosh D, Shah R, Varambally S, Kurachi K, Pienta KJ, Rubin MA, Chinnaiyan AM (2001) *Nature* 412:822–826.
10. List K, Szabo R, Molinolo A, Sriuranpong V, Redeye V, Murdock T, Burke B, Nielsen BS, Gutkind JS, Bugge TH (2005) *Genes Dev* 19:1934–1950.
11. Takeuchi T, Shuman MA, Craik CS (1999) *Proc Natl Acad Sci USA* 96:11054–11061.
12. Fraser HB, Hirsh AE, Wall DP, Eisen MB (2004) *Proc Natl Acad Sci USA* 101:9033–9038.
13. Miki R, Kadota K, Bono H, Mizuno Y, Tomaru Y, Carninci P, Itoh M, Shibata K, Kawai J, Konno H, *et al.* (2001) *Proc Natl Acad Sci USA* 98:2199–2204.
14. Lin CY, Anders J, Johnson M, Dickson RB (1999) *J Biol Chem* 274:18237–18242.
15. Choe Y, Leonetti F, Greenbaum DC, Lecaille F, Bogyo M, Bromme D, Ellman JA, Craik CS (2006) *J Biol Chem* 281:12824–12832.
16. Friedrich R, Fuentes-Prior P, Ong E, Coombs G, Hunter M, Oehler R, Pierson D, Gonzalez R, Huber R, Bode W, Madison EL (2002) *J Biol Chem* 277:2160–2168.
17. Zhou YQ, He C, Chen YQ, Wang D, Wang MH (2003) *Oncogene* 22:186–197.
18. Skeel A, Leonard EJ (2001) *J Biol Chem* 276:21932–21937.
19. Leonard EJ *Ciba Found Symp* 212:183–191, 1997; discussion 192–197.
20. Wang MH, Skeel A, Leonard EJ (1996) *J Clin Invest* 97:720–727.
21. Wang MH, Yoshimura T, Skeel A, Leonard EJ (1994) *J Biol Chem* 269:3436–3440.
22. Skeel A, Yoshimura T, Showalter SD, Tanaka S, Appella E, Leonard EJ (1991) *J Exp Med* 173:1227–1234.
23. Wang MH, Cox GW, Yoshimura T, Sheffler LA, Skeel A, Leonard EJ (1994) *J Biol Chem* 269:14027–14031.
24. Wang MH, Dlugosz AA, Sun Y, Suda T, Skeel A, Leonard EJ (1996) *Exp Cell Res* 226:39–46.
25. Wang MH, Julian FM, Breathnach R, Godowski PJ, Takehara T, Yoshikawa W, Hagiya M, Leonard EJ (1997) *J Biol Chem* 272:16999–17004.
26. Tam EM, Morrison CJ, Wu YI, Stack MS, Overall CM (2004) *Proc Natl Acad Sci USA* 101:6917–6922.
27. Zhou Q, Snipas S, Orth K, Muzio M, Dixit VM, Salvesen GS (1997) *J Biol Chem* 272:7797–7800.
28. Oberst MD, Chen LY, Kiyomiya KI, Williams CA, Lee MS, Johnson MD, Dickson RB, Lin CY (2005) *Am J Physiol Cell Physiol* 289:C462–C470.
29. Takeuchi T, Harris JL, Huang W, Yan KW, Coughlin SR, Craik CS (2000) *J Biol Chem* 275:26333–26342.
30. Bhatt AS, Erdjument-Bromage H, Tempst P, Craik CS, Moasser MM (2005) *Oncogene* 24:5333–5343.
31. Chen YQ, Zhou YQ, Fu LH, Wang D, Wang MH (2002) *Carcinogenesis* 23:1811–1819.
32. List K, Haudenschild CC, Szabo R, Chen W, Wahl SM, Swaim W, Engelholm LH, Behrendt N, Bugge TH (2002) *Oncogene* 21:3765–3779.
33. Chen YQ, Zhou YQ, Fisher JH, Wang MH (2002) *Oncogene* 21:6382–6386.
34. Welm AL, Sneddon JB, Taylor C, Nuyten D, van de Vijver M, Hasegawa BH, Bishop MJ *Proc Natl Acad Sci USA*, in press.
35. Coussens LM, Werb Z (2002) *Nature* 420:860–867.
36. Harris JL, Backes BJ, Leonetti F, Mahrus S, Ellman JA, Craik CS (2000) *Proc Natl Acad Sci USA* 97:7754–7759.
37. Benjamini Y, Hochberg Y (1995) *J R Stat Soc* 57:289–300.
38. Sun J, Pons J, Craik CS (2003) *Biochemistry* 42:892–900.